ISSN 1068-3712, Russian Electrical Engineering, 2024, Vol. 95, No. 2, pp. 156–163. © Allerton Press, Inc., 2024.
Russian Text © The Author(s), 2023, published in Vestnik Ivanovskogo Gosudarstvennogo Energeticheskogo Universiteta Imeni V.I. Lenina, 2023, No. 4, pp. 46–53.

A Parametric Model of a Synchronous Reluctance Motor with a TLA Rotor in Steady-State and Transient Modes

V. N. Karaulov[a], * and A. F. Dorzhinkevich[a], **

[a] *Lenin Ivanovo State Energy University, Ivanovo, 153003 Russia*

**e-mail: karaulov@em.ispu.ru*

***e-mail: dorzhinkevichanatol@gmail.com*

Received March 12, 2023; revised June 7, 2023; accepted November 25, 2023

Abstract—There is significant practical and scientific interest in synchronous reluctance motors with a transversally laminated anisotropic (TLA) rotor. TLA rotor core has a transverse lamination, internal grooves and highly saturated areas. The configuration of rotor slots is complex and varied. It is an urgent task to develop a parametric model of a synchronous reluctance motor with a TLA rotor designed to calculate steady-state and transient engine operating conditions. A classical parametric model of a synchronous reluctance motor is used that is based on the theory of two reactions. The presented method for calculating the parameters of a model of a synchronous reluctance motor with a TLA rotor is based on the results of a field calculation of two static states of a magnetic field. Calculations of steady-state conditions of a synchronous reluctance motor are performed according to engineering formulas, which are obtained from the equation of voltage equilibrium in the stator phase. To calculate the transient modes of a synchronous reluctance motor, the Park—Gorev equations were used. Field models of the synchronous reluctance motor under study are presented for axial and transverse rotor positions. The magnetic field's main harmonics in the gap and their dependences on the armature current are calculated. Formulas are given for calculating the armature winding inductive parameters and a synchronous reluctance motor operating characteristics. Differential equations used to calculate processes in a synchronous reluctance motor are presented. Using a parametric model, the operating characteristics of a synchronous reluctance motor, the process of frequency starting, and the electromechanical process of a synchronous reluctance motor's operation with an asymmetrical power supply are calculated. Calculation results are compared with the field modeling results of a synchronous reluctance motor with a TLA rotor in the Ansys Maxwell environment. The classical parametric model of a synchronous machine based on the theory of two reactions allows one to quickly and accurately analyze the steady-state and transient operating conditions of a synchronous reluctance motor with a TLA rotor under various power and mechanical load conditions, including abnormal ones.

Keywords: synchronous reluctance motor, operating characteristics of synchronous reluctance motor, transversally laminated anisotropic rotor, parametric model, steady-state engine operating conditions, transient engine operating conditions

DOI: 10.3103/S1068371224700111

INTRODUCTION

Synchronous reluctance motors (SRMs) with a transversally laminated anisotropic (TLA) rotor have become more widespread in automatic control systems [1, 2]. The advantages of SRMs are low cost, high efficiency, ability to accurately control speed over a wide range [3], and small torque pulsations [4]. In [5–7], it is shown that the energy efficiency and energy intensity of SRMs are greater than those of asynchronous motors. The design features of the SRMs are that the TLA rotor core has a transverse lamination, internal grooves, and highly saturated areas. The configuration of grooves in various SRMs is complex and varied. In [8, 9] and in many other works, it is shown that, to control SRMs, it is advisable to use the a parametric model of the engine, the parameters of which should be calculated taking into account the saturation of steel sections.

In [10], it was proposed to calculate the SRM parameters based on the parameters of an asynchronous motor, the stator of which corresponds to the stator of SRM being considered. When calculating the parameters of an asynchronous motor's equivalent circuit, its catalog data were used. In [11], it is shown that, when constructing of a control systems for a reluctance electric machine, it is necessary to take into account the change in the values of an armature winding's parameters during an electric drive operation. An algorithm for identifying parameters in a stationary mode of machine operation has been obtained. In [12,

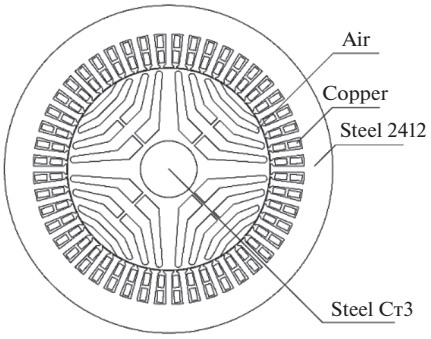

Fig. 1. Design of SRM with a TLA rotor.

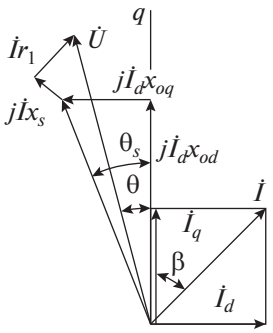

Fig. 2. SRM vector diagram.

13], an analysis and optimization of SRM's rotor design was carried out based on calculations of the SRM's electromagnetic field in the machine's stationary operating mode. In [14], the SRM inductive parameters were calculated based on electromagnetic field's calculations.

Developing a parametric model of an SRM with a TLA rotor intended for calculating steady-state and transient engine operating conditions is an urgent task. The SRM model parameters should be determined based on the electromagnetic field calculations, which makes it possible to take into account the machine's design features and changes in the saturation of a magnetic circuit depending on the armature current magnitude.

When modeling processes in an SRM with a TLA rotor, a classical SRM model based on the theory of two reactions can be used. A method is given below for calculating model parameters based on the results of field calculations of two static states of a magnetic field, a field models of the investigated SRM at axial and transverse rotors' positions are described, the main harmonic magnetic fields in the gap and their dependence on the armature current are calculated, and formulas for calculating the inductive parameters of an armature winding are given.

To calculate the steady-state operating modes of an SRM with a TLA rotor, engineering formulas were used obtained on the basis of the voltage equilibrium equation in the stator phase, in addition to calculations of transient regimes being performed based on the Park–Gorev equations. Using a parametric model, the SRM operating characteristics, the process of frequency starting, and the electromechanical process of SRM operation with an unbalanced power supply were calculated. The calculation results are compared with the field modeling results of a synchronous reluctance motor with a TLA rotor in the Ansys Maxwell environment.

MATERIALS AND METHODS

Figure 1 shows the design of a synchronous reluctance motor being studied with a TLA rotor. The engine technical parameters were a rated power of 75 kW, rated phase voltage of 380 V, rated phase current of 86 A, rated speed 1500 of rpm, three phases, and supply voltage frequency of 50 Hz.

SRM Parametric Model

The model for the steady-state synchronous operating mode of an SRM is the voltage equilibrium equation in the stator phase for the effective values of voltages and currents on the space–time complex plane:

$$\dot{U} = j\dot{I}_d x_{ad} + j\dot{I}_q x_{aq} + j\dot{I}x_s + \dot{I}r_1. \quad (1)$$

This equation corresponds to the vector diagram of the SRM presented in Fig. 2.

Model of SRM in transient operating modes is the system of Park–Gorev differential equations written in the d, q, 0 axes (the d axis leads the q axis):

$$\begin{gathered} u_d = \frac{d\Psi_d}{dt} + i_d r_1 + \psi_q \omega; \\ u_q = \frac{d\Psi_q}{dt} + i_q r_1 - \psi_d \omega; \\ u_0 = i_0 r_1 + L_{\sigma 1}\frac{di_0}{dt}; \\ M_{\text{em}} = M_{\text{в}} + J\frac{d\Omega}{dt}; \\ M_{\text{em}} = 1.5p(i_d\psi_q - i_q\psi_d); \\ \psi_d = \frac{x_d(I)}{\omega} I_d, \quad \psi_q = \frac{x_q(I)}{\omega} I_q. \end{gathered} \quad (2)$$

The resistances used in Eqs. (1) and (2) are the parameters of SRM with TLA rotor. The inductive reactances of armature reaction along the axial and transverse axes x_{ad} and x_{aq} depend on the TLA rotor's

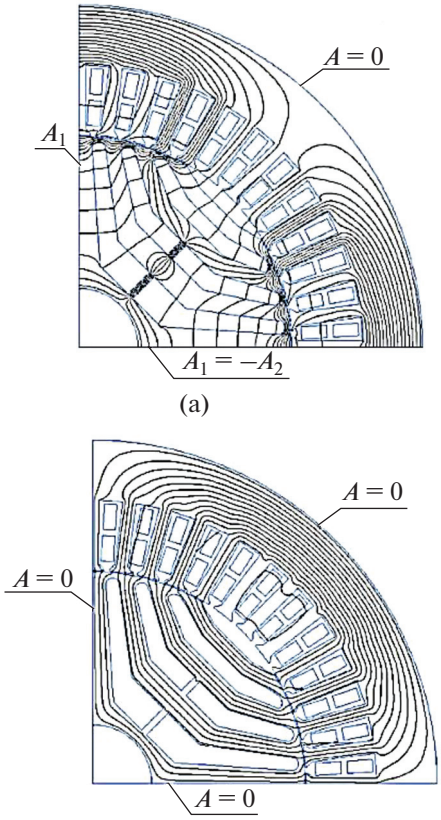

Fig. 3. Field models of SRM for two rotor positions: (a) transverse position; (b) axially position.

design, the magnetic circuit's saturation, and, accordingly, the armature current's magnitude.

RESULTS

Calculation of Parameters of an SRM with a TLA Rotor

To determine dependences $x_{ad} = f(I_d)$, $x_{aq} = f(I_q)$, a field calculation of the magnetic field's two static states was performed—for the rotor's transverse and axial positions (Fig. 3).

Figure 3 shows the boundary conditions for the vector magnetic potential and the magnetic induction line. On the armature's outer diameter and for the sides of an axial field model, the Dirichlet boundary condition is chosen; for the transverse field model's lateral sides, the condition of odd periodicity is chosen.

Figures 4 and 5 present the results of field calculations: the magnetic induction wave on the working gap's middle line and its first harmonic wave at the magnetic circuit's different saturation.

Figure 6 shows the amplitude's dependences of the first spatial harmonic of magnetic induction in the gap on the armature phase current $B_{d1} = f(I_d)$ and $B_{q1} = f(I_q)$.

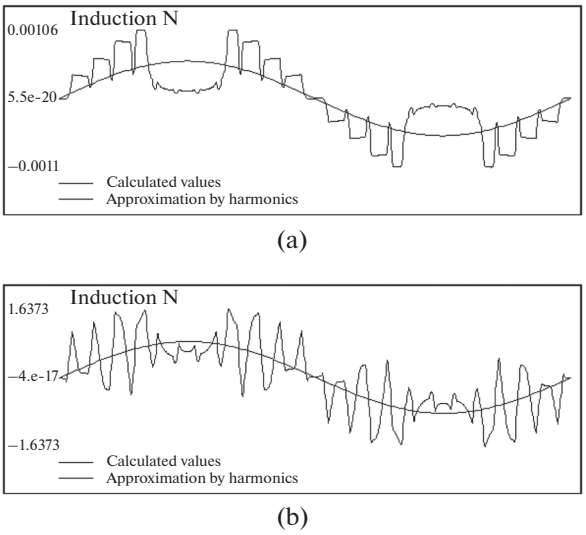

Fig. 4. Transverse wave of magnetic induction in the working gap and its first harmonic B_{q1}: (a) in the absence of saturation in the magnetic circuit; (b) at maximum saturation of the magnetic circuit.

Dependences $B_{d1} = f(I_d)$ and $B_{q1} = f(I_q)$ are used to calculate the inductive reactance of an armature reaction. The following are calculated:

• axial and transverse armature fluxes, Wb:

$$\Phi_{ad} = \frac{2}{\pi} B_{d1} l_\delta \tau; \quad \Phi_{aq} = \frac{2}{\pi} B_{q1} l_\delta \tau;$$

• axial and transverse EMF of an armature reaction, V:

$$E_{ad} = \sqrt{2}\pi f_1 w k_r \Phi_{ad};$$
$$E_{aq} = \sqrt{2}\pi f_1 w k_r \Phi_{aq};$$

• inductive resistance of armature reaction, Ω:

$$x_{ad} = \frac{E_{ad}}{I_d}; \quad x_{aq} = \frac{E_{aq}}{I_q};$$

• armature winding inductive leakage resistance, Ω:

$$x_\sigma = 1.58 \frac{f}{100} \left(\frac{w_1}{100}\right)^2 \frac{l_\delta}{pq} (\lambda_P + \lambda_F + \lambda_D);$$

• armature synchronous inductive resistance, Ω:

$$x_d = x_{ad} + x_\sigma; \quad x_q = x_{aq} + x_\sigma.$$

As a result, the dependences of resistance on armature current were obtained:

$$x_d = f(I_d); \quad x_q = f(I_q). \qquad (3)$$

Performance Calculation

To calculate the SRM's performance characteristics, Eq. (1) is used. Angle Θ is chosen as an independent

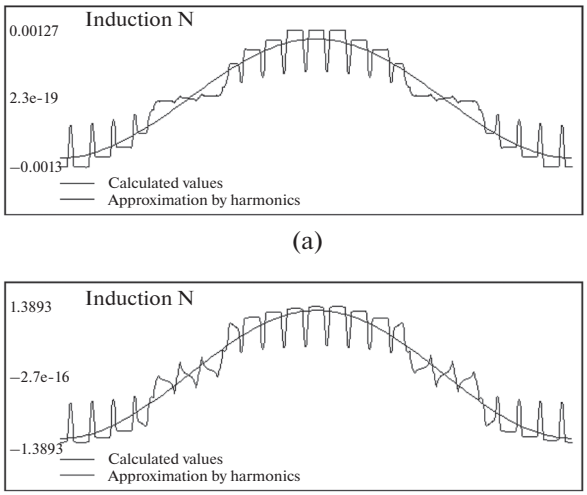

Fig. 5. Axial wave of magnetic induction in the working gap and its first harmonic B_{d1}: (a) in the absence of saturation in the magnetic circuit; (b) at maximum saturation of the magnetic circuit.

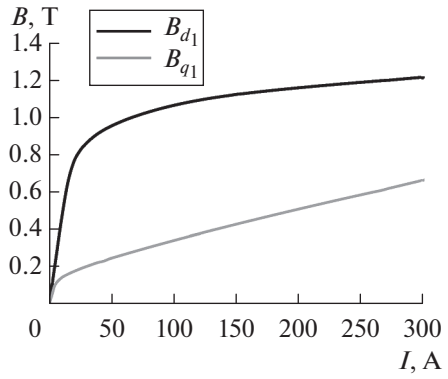

Fig. 6. Dependences of amplitude of the first spatial harmonic magnetic induction in the gap on armature phase current $B_{d1} = f(I_d)$ and $B_{q1} = f(I_q)$.

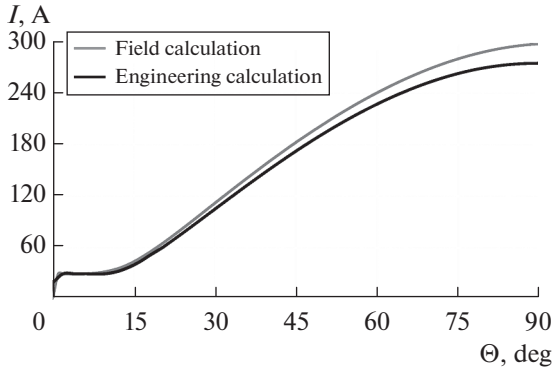

Fig. 7. Dependence of effective armature current on load angle $I = f(\Theta)$.

variable—the angle between supply voltage vector U and transverse axis q, which is shown in Fig. 2. Performance is based on load angle Θ ranging from 0° to 90°.

From the vector diagram presented in Fig. 2, the formulas are obtained for calculating an axial and transverse armature currents, A:

$$I_d = \frac{U_{\text{ph}}\left(x_q(I)\cos(\Theta) - r_1\sin(\Theta)\right)}{r_1^2 + x_d(I)x_q(I)};$$
$$I_q = \frac{U_{\text{ph}}\left(x_d(I)\sin(\Theta) + r_1\cos(\Theta)\right)}{r_1^2 + x_d(I)x_q(I)}. \quad (4)$$

Currents calculated using formulas (4) are used to clarify the values of inductive reactances using dependences $x_d = f(I_d)$ and $x_q = f(I_q)$. Current calculations and resistance refinement are repeated until the current values in the current and previous iterations no longer differ.

The following are calculated:

- armature phase current, A:

$$I = \sqrt{I_q^2 + I_d^2};$$

- reactive torque, N m:

$$M = \frac{mpU_{\text{ph}}^2}{2\omega}\left(\frac{1}{x_q} - \frac{1}{x_d}\right)\sin(2\Theta);$$

- active power consumption, W:

$$P_1 = \frac{mU_{\text{ph}}^2(x_d - x_q)}{2(r_1^2 + x_d x_q)}\sin(2\Theta) + \frac{mU_{\text{ph}}^2 r_1}{r_1^2 + x_d x_q};$$

- electromagnetic efficiency, %:

$$\eta = \frac{P_{\text{em}}}{P_1}\times 100;$$

- power factor, rel. units:

$$\cos\varphi = \frac{P_1}{mU_{\text{ph}}I}. \quad (5)$$

Figures 7–11 present the performance characteristics of SRMs studied with a TLA rotor calculated using formulas (4)–(5), as well as analogous characteristics obtained as a result of field calculations in Ansys Maxwell.

Calculation of Transient Processes in an SRM

Transient processes in an SRM are calculated by numerical integration of system of differential equations (2). Dependences of the instantaneous values of an axial and transverse armature currents on the corresponding flux linkages are used. These dependences $i_d = f(\psi_d)$ and $I_q = f(\psi_q)$ are shown in Fig. 12. They are determined at the stage of calculating the SRM parameters.

Table 1. Energy indicators in steady-state operation

Energy indicators	Engineering calculation	Field calculation
η, rel. units	0.977	0.971
cosφ, rel. units	0.771	0.732

Table 2. Energy indicators in steady-state operation with unbalanced power supply

Energy indicators	Engineering calculation	Field calculation
η, rel. units	0.974	0.964
cosφ, rel. units	0.74	0.728

Calculation of the electromechanical process of an SRM's frequency starting with a TLA rotor has been carried out. Scalar control of the starting process is implemented: the amplitude and frequency of supply voltage linearly increase to nominal values within one second and then do not change. At moment of time $t = 1.5$ s, there is a "surge" of the rated load M_n = 478 N m. The braking torque magnitude depends on the rotor's angular speed according to the nature of a fan load:

$$M_F = M_n\left(\frac{\omega}{\omega_n}\right)^2.$$

Steel and mechanical losses were not taken into account. Calculation results of the SRM parametric model (engineering calculation) are compared with similar results of field calculations. Figure 13 shows the change in rotor speed during the process of SRM frequency starting, Fig. 14 shows the change in electromagnetic moment, and Fig. 15 shows the change in current in the armature phase.

The machine's energy indicators are calculated after the start-up process is completed using the following formulas:

$$\eta = \frac{P_2}{P_1} = \frac{\frac{1}{T}\int_{t_c-T}^{t_c}(M\omega)dt}{\frac{1}{T}\int_{t_c-T}^{t_c}(u_A i_A + u_B i_B + u_C i_C)dt};$$

$$\cos\varphi = \frac{P_1}{S_1} = \frac{\frac{1}{T}\int_{t_c-T}^{t_c}(u_A i_A + u_B i_B + u_C i_C)dt}{U_A I_A + U_B I_B + U_C I_C}.$$

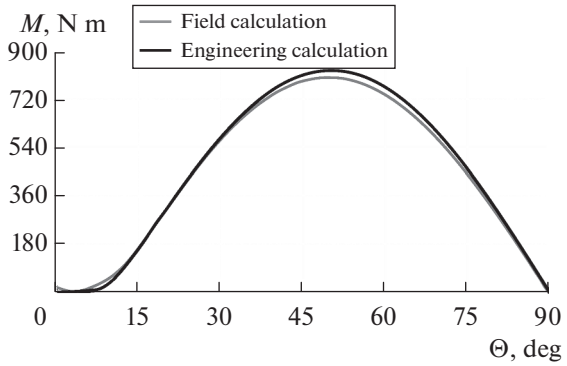

Fig. 8. Dependence of electromagnetic torque on load angle $M = f(\Theta)$.

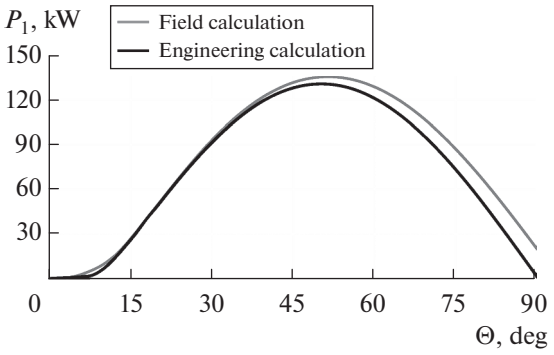

Fig. 9. Dependence of active power consumption on load angle $P_1 = f(\Theta)$.

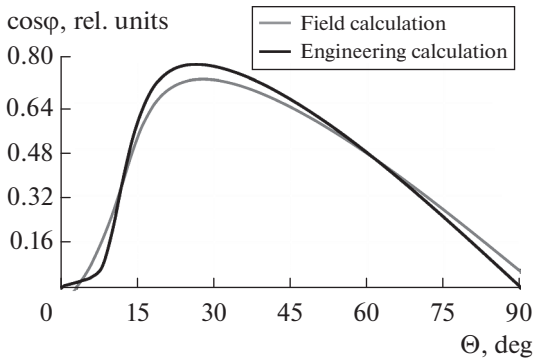

Fig. 10. Dependence of power factor on load angle $\cos\varphi = f(\Theta)$.

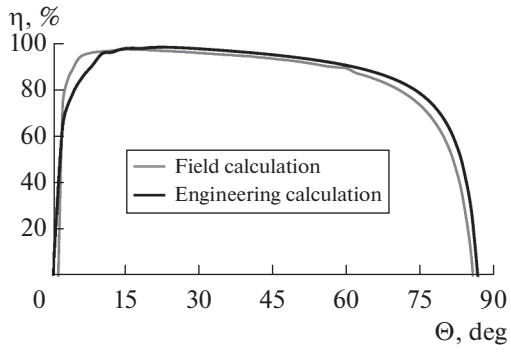

Fig. 11. Dependence of efficiency on load angle $\eta = f(\Theta)$.

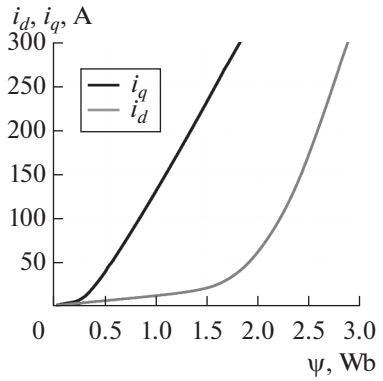

Fig. 12. Dependences of instantaneous currents on instantaneous flux linkages $i_d = f(\psi_d)$ and $I_q = f(\psi_q)$.

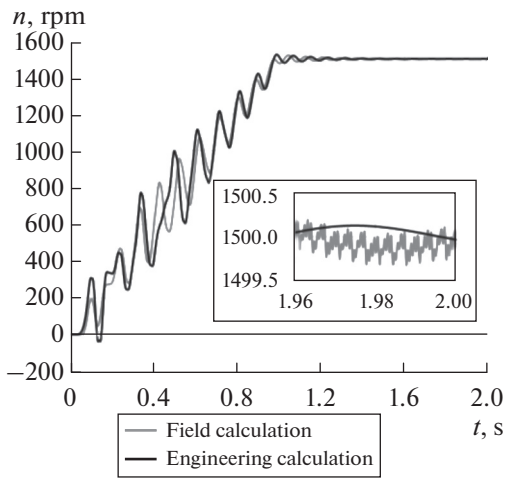

Fig. 13. Rotor speed during frequency starting.

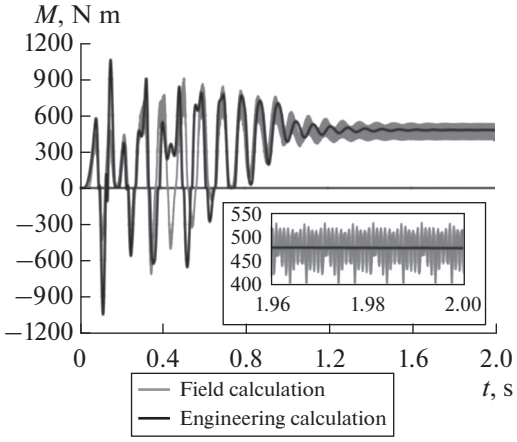

Fig. 14. Electromagnetic torque during frequency starting.

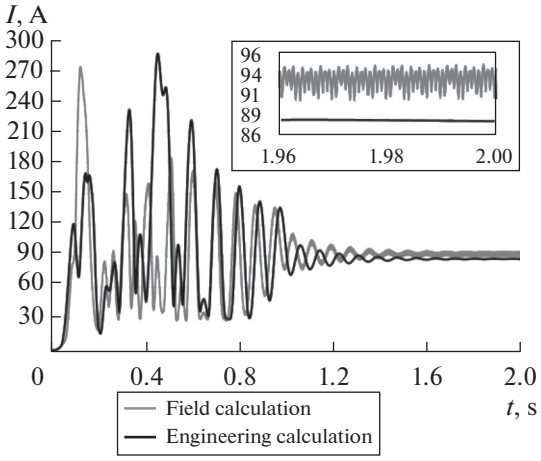

Fig. 15. Effective armature current during frequency starting.

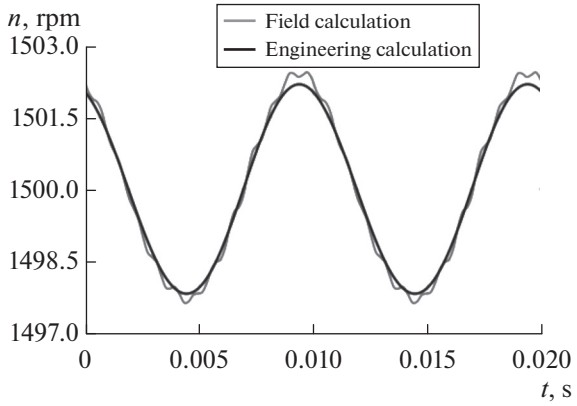

Fig. 16. Rotor speed with asymmetrical supply voltage.

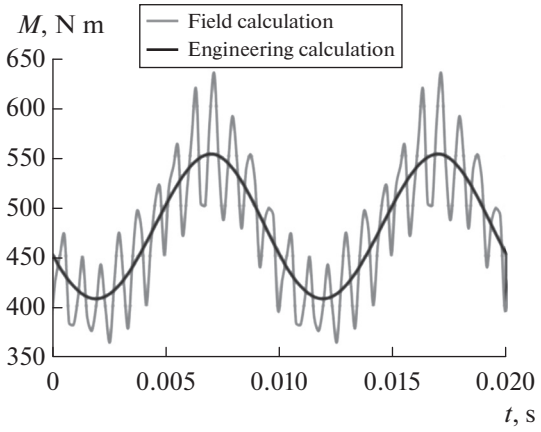

Fig. 17. Electromagnetic torque with asymmetrical supply voltage.

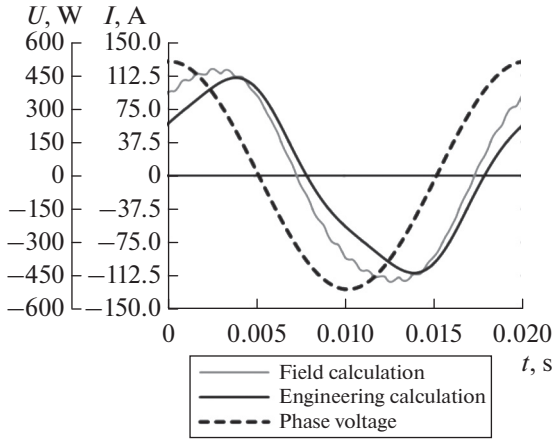

Fig. 18. Voltage and current in the stator phase with an asymmetrical supply voltage.

Calculation of Asymmetric SRM Operating Modes

Transient and steady-state processes in asymmetrical operating modes of the SRM are calculated by numerically solving system of equations (2).

Figures 16–18 and Table 2 present the results of calculating the steady-state electromechanical process of operation of an SRM with a TLA rotor with an unbalanced supply: in one of the phases, the amplitude and phase of voltage are changed by 5%. The parametric model calculation results for an SRM (engineering calculation) are compared with the similar results of field calculations.

CONCLUSIONS

A synchronous machine classical parametric model based on the theory of two reactions, as well as a method for calculating model parameters based on the results of field calculations of two static states of the magnetic field, allows one to quickly and efficiently analyze the steady-state and transient operating modes of a synchronous reluctance motor with a TLA rotor under various conditions of power supply and mechanical load, including abnormal ones.

FUNDING

This work was supported by ongoing institutional funding. No additional grants to carry out or direct this particular research were obtained.

CONFLICT OF INTEREST

The authors of this work declare that they have no conflicts of interest.

REFERENCES

1. Shul'ga, R.N., Synchronous reluctance engine in a private electric drive, *Elektrooborudov.: Ekspluatatsiya Remont*, 2023, no. 1, pp. 44–55.
2. Tikhomirov, O.I., Synchronous reluctance motors for cre-ating energy-efficient solutions of class IE5, *Avtom. Prom-sti*, 2022, no. 1, pp. 42–44. https://doi.org/10.25728/avtprom.2022.01.09
3. Mitrofanov, I.I., Optimal control of the angular velocity of a synchronous jet engine in terms of accuracy, *Izv. Tul. Gos. Univ. Tekh. Nauki*, 2012, no. 11-1, pp. 186–190.
4. Ptakh, G.K., Comparative evaluation of alternating current electric motors of asynchronous and synchronous types for the purpose of their application in rowing electrical installations of icebreakers of high power, *Izv. Vyssh. Uchebn. Zaved., Elektromekh.*, 2019, vol. 62, no. 5, pp. 24–30. https://doi.org/10.17213/0136-3360-2019-5-24-30
5. Zakharov, A.V., Malafeev, S.I., and Dudulin, A.L., Synchronous reluctance motor: Design and experimental research, *2018 X Int. Conf. on Electrical Power Drive Systems (ICEPDS)*, Novocherkassk, 2018, IEEE, 2018, pp. 1–4. https://doi.org/10.1109/icepds.2018.8571500
6. Murataliyev, M., Degano, M., Di Nardo, M., Bianchi, N., and Gerada, C., Synchronous reluctance machines: A comprehensive review and technology comparison, *Proc. IEEE*, 2022, vol. 110, no. 3, pp. 382–399. https://doi.org/10.1109/jproc.2022.3145662
7. Paramonov, A.S., Kazakbaev, V.M., Oshurbekov, S.Kh., and Prakht, V.A., Comparison of power consumption of asynchronous and synchronous jet engines in a pumping application, *Energo- i resursosberezhenie. Energoobespechenie. Netraditsionnye i vozobnovlyaemye istochniki energii. Atomnaya energetika. Materialy Mezhdunar. nauch.-prakt. konf. stud., asp. i molodykh uchenykh, posvyashchennoi pamyati prof. Danilova N.I. (1945–2015) – Danilovskikh chtenii* (Proc. Int. Sci. and Pract. Conf. of Students, Postgraduates and Young Scientists Dedicated to the Memory of Prof. N.I. Danilov (1945–2015) Energy and Resource Conservation. Energy Supply. Unconventional and Renewable Energy Sources. Nuclear Power Engineering (Danilovsky Readings)), Yekaterinburg: 2019, pp. 300–303.
8. Han, Ya., Wu, X., He, G., Hu, Yi., and Ni, K., Nonlinear magnetic field vector control with dynamic-variant parameters for high-power electrically excited synchronous motor, *IEEE Trans. Power Electron.*, 2020, vol. 35, no. 10, pp. 11053–11063. https://doi.org/10.1109/tpel.2020.2977390
9. Choi, J.-S., Ko, J.-S., and Chung, D.-H., Efficiency optimization control of SynRM drive, *2006 SICE-ICASE Int. Joint Conf.*, Busan, Korea (South), 2006, IEEE, 2006, pp. 690–695. https://doi.org/10.1109/sice.2006.315625
10. Kazakbaev, V.M., Prakht, V.A., and Dmitrievskiy, V.A., Calculation of the performance characteristics of a synchronous jet engine in a pump drive, *Aktual'nye problemy energosberegayushchikh elektrotekhnologii (APEET-2014), Materialy III Mezhdunar. konf.* (Actual Problems of Energy Saving Electrical Technologies (APEET-2014): Proc. 3rd Int. Conf.), Yekaterinburg: Ural. Fed. Univ.

im. Pervogo Prezidenta Rossii B.N. El'tsina, 2014, pp. 238–243.

11. Samoseyko, V.F., Sharashkin, S.V., and Gel'ver, F.A., Identification of parameters of a reactive electric motor with anisotropic magnetic conductivity of the rotor, *Vestn. Gos. Univ. Morskogo Rechnogo Flota Imeni Admirala S.O. Makarov*, 2017, vol. 9, no. 3, pp. 637–644. https://doi.org/10.21821/2309-5180-2017-9-3-637-644
12. Tursini, M., Villani, M., Fabri, G., Credo, A., Parasiliti, F., and Abdelli, A., Synchronous reluctance motor: Design, optimization and validation, *2018 Int. Symp. on Power Electronics, Electrical Drives, Automation and Motion (SPEEDAM)*, Amalfi, Italy, 2018, IEEE, 2018, pp. 1297–1302. https://doi.org/10.1109/speedam.2018.8445304
13. Barta, J. and Ondrusek, C., Rotor design and optimization of synchronous reluctance machine, *MM Sci. J.*, 2015, no. 1, pp. 555–559. https://doi.org/10.17973/mmsj.2015_03_201504
14. Suvorkova, E.E., Dement'ev, Yu.N., and Burul'ko, L.K., Calculation of magnetic fields and inductive parameters of synchro-nous jet engines, *Fundam. Issled.*, 2016, no. 6-1, pp. 112–116.

Translated by V. Selikhanovich